

1 **Supporting Information**

2 **Interpreting UniFrac with Absolute Abundance: A Conceptual and Practical Guide**

3 Augustus Pendleton<sup>1\*</sup> & Marian L. Schmidt<sup>1\*</sup>

4 <sup>1</sup>Department of Microbiology, Cornell University, 123 Wing Dr, Ithaca, NY 14850, USA

5 Corresponding Authors: Augustus Pendleton: [arp277@cornell.edu](mailto:arp277@cornell.edu); Marian L. Schmidt:  
6 [marschmi@cornell.edu](mailto:marschmi@cornell.edu)

7

8 **Supporting Methods**

9 *ASV Generation and Phylogenetic Tree Construction*

10 Sequencing data and identifying metadata were downloaded from the Sequence Read  
11 Archive (SRA), from BioProject IDs PRJNA815056, PRJNA575097, PRJNA1212049, and  
12 PRJNA302180 [1–4]. Full details and code of the Pendleton et al. 2025 data analysis are  
13 included within that paper and associated Github repository and not shown here. Each dataset  
14 varied substantially in terms of which 16S region it targeted, sequencing strategy, and read  
15 quality, so ASV generation varied between them in terms of primer removal, filtering, and  
16 trimming (see code for full description of these steps). Post trimming, all ASVs were generated  
17 using the same methods within the standard DADA2 workflow [5]. Chimaeras were removed,  
18 and ASVs were size selected (252/253 bp for V4 datasets, >400bp for V3-V4 datasets).  
19 Taxonomy was assigned via the Silva v138.2 database, and used to remove mitochondrial and  
20 chloroplast sequences [6]. When sequencing positives or negatives were present, they were  
21 removed.

22 Phylogenetic trees were built using alignment via MAFFT followed by FastTree under a  
23 generalized time-reversible model [7, 8]. Trees were visualized via ggtree in R, and anomalously  
24 long branches were removed using ape [9]. Trees, metadata, taxonomy, and ASV abundances  
25 (OTU tables) were organized and analyzed using phyloseq [10].

26 *Rarefaction and  $\beta$ -diversity*

27 To generate rarefied ASV tables of equal sequencing depth, ASV abundance matrices  
28 were subsampled using a multivariate hypergeometric distribution via the rmvhyper function in  
29 the extraDistr package (see generate\_rarefied\_abs\_tables.R) [11]. Each ASV was then converted  
30 to relative abundances, and then to absolute abundances by multiplying the relative abundance  
31 by each samples cell count or 16S copy number. Bray-Curtis dissimilarities were calculated via  
32 the vegdist function in vegan [12]. Unless otherwise noted, all Unifrac distances were calculated  
33 via the GUnifrac package [13]. Final distance matrices were the average of all rarefied distance  
34 matrices. All samples within each dataset were used for contour plots in Figure 2.

35 *PERMANOVAs and Ordinations*

36 PERMANOVAs were conducted via the adonis2 function in vegan (Fig. 3 and Fig. S2).  
37 To limit confounding variables, not all samples were used in these analyses. From the cooling  
38 water dataset, just samples from Reactor cycle 1 were used. For the mouse gut, just stool samples  
39 were used. For the soil dataset, just mature samples were used. All PERMANOVAs were run  
40 with 1,000 iterations. These same, simplified datasets were used for Principal Coordinates  
41 Analysis in Fig S3.

42 *Timing Analysis*

43 To estimate computational time, we subsampled the soil dataset to a set number of ASVs,  
44 samples, and  $\alpha$  numbers. When testing ASV number, we used 10 samples and one  $\alpha$  value, when  
45 testing sample or  $\alpha$  values, ASVs were held constant at 2,000. Each case was replicated 20  
46 times, and computation time was calculated via the microbenchmark function from the  
47 microbenchmark package, with two replications each time [14].

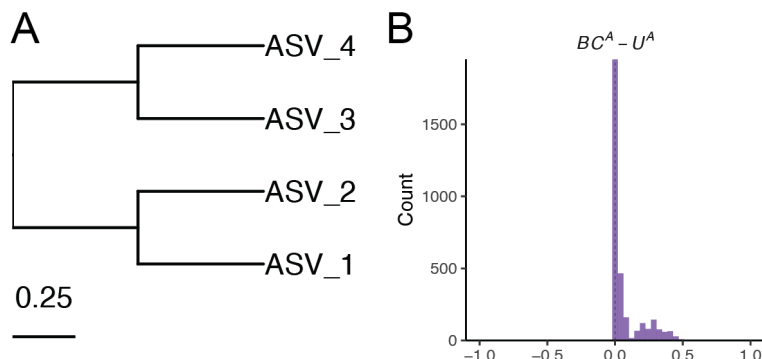
48 *Error Analysis*

49 To estimate the impact of random error on quantification methods, we used the mouse  
50 gut dataset, focusing only on the stool samples. These samples ranged in 16S copy number from  
51  $10^{11}$ - $10^{12}$  copies/gram. We tested a range of potential error, from 1% up to 50%. For each error  
52 percentage, the amount of error was selected from a normal distribution with a mean of that error  
53 percent and a standard deviation  $1/10^{\text{th}}$  of that error percentage. This error was then randomly  
54 assigned a direction (by multiplying by a binomial distribution of -1 and 1), and multiplied by  
55 the copy number to create a deviation from the true value, which was added to the original value.  
56 For example, in the case of 50% error, we first drew a random selection of error values from a  
57 distribution with mean 0.5 and standard deviation of 0.05. These errors were then randomly  
58 assigned to be negative or positive, and multiplied by the original cell counts, plus the cell count  
59 itself. We repeated this fifty times. Across these fifty iterations, we first rarefied the ASV  
60 abundances to relative abundance and then normalized to absolute abundance using these error-  
61 added values. We then compared the absolute difference in  $GU^A$  or  $BC^A$  from these error-added  
62 datasets compared to the original data to produce Fig. 4C-D.

63 *Other Coding Packages*

64 Other packages used for general coding and visualization include tidyverse, purr,  
65 patchwork, NatParksPalette, broom, corrr, ggpibr, and renv. All packages and version numbers  
66 are listed in Table S1.

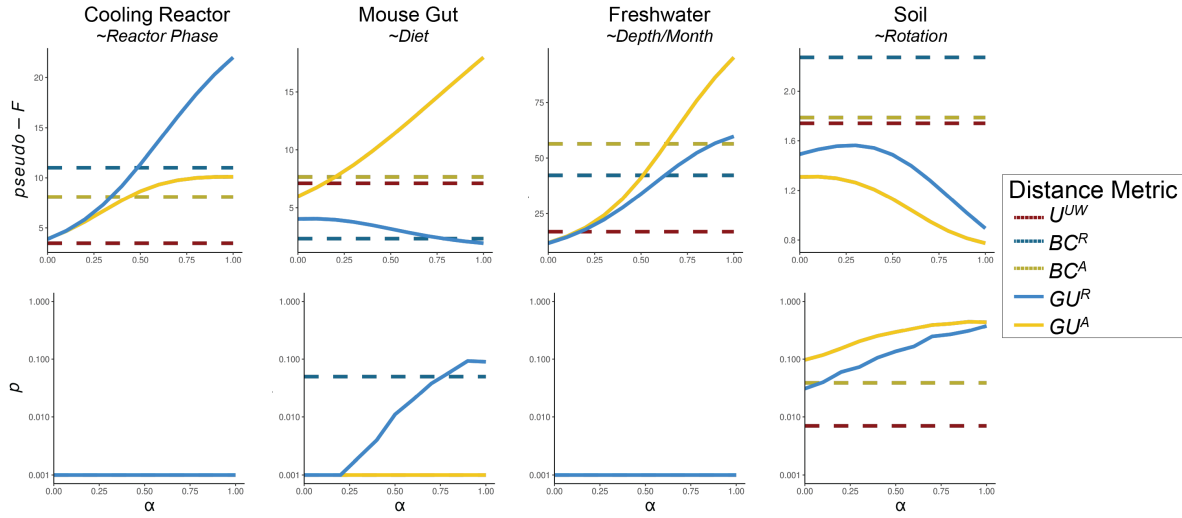
67 **Supplemental Figures**



68

69 *Figure S1.*  $U^A$  is always less than  $BC^A$  when branch lengths are fully symmetrical. (A)  
70 Symmetrical tree used for simulations as opposed to non-symmetrical tree in Fig. 1A. (B)  
71 Distribution of differences between  $BC^A$  and  $U^A$ . As the differences are never negative,  $U^A$  is  
72 always less than or equal to  $BC^A$ .

73

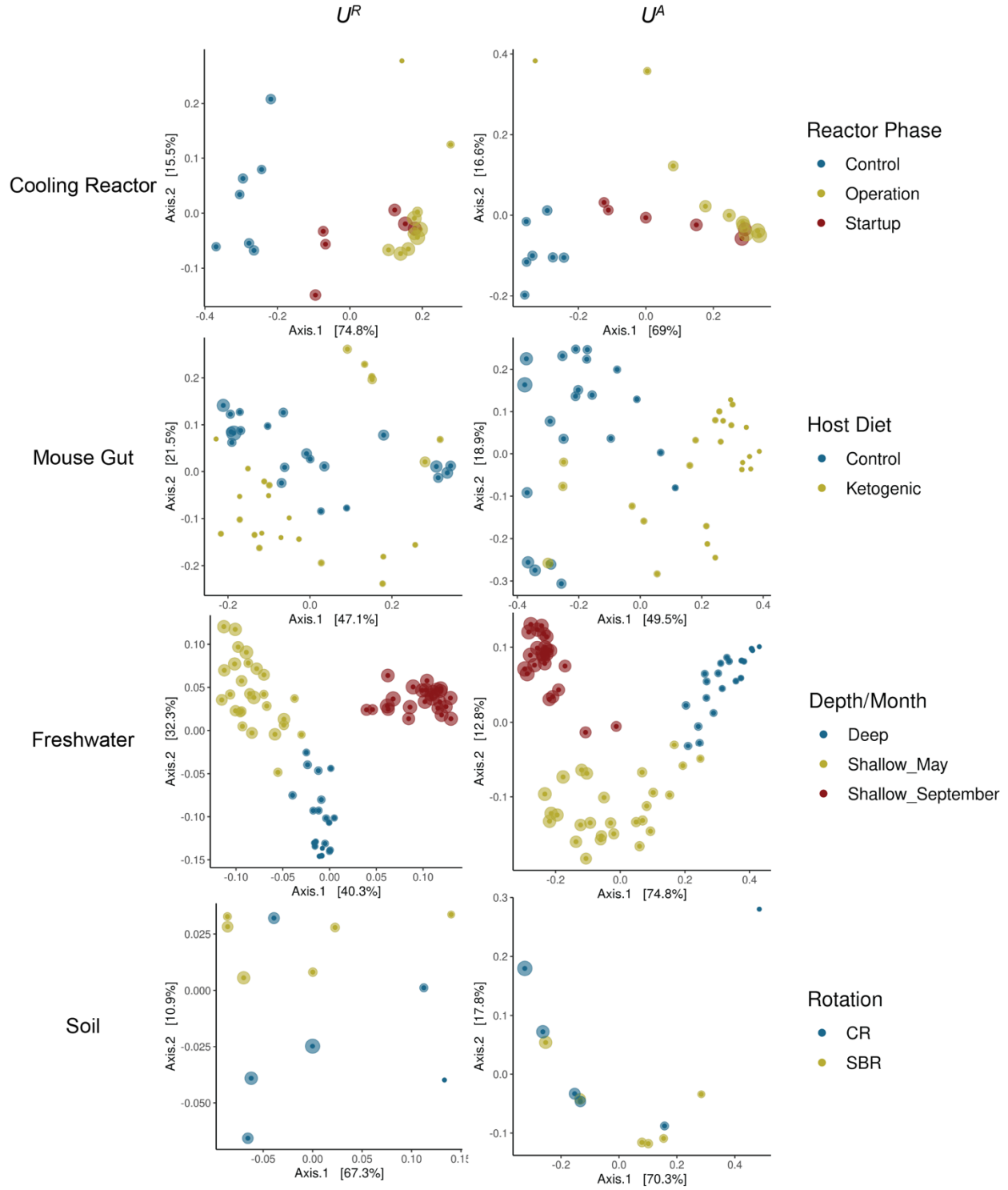


74

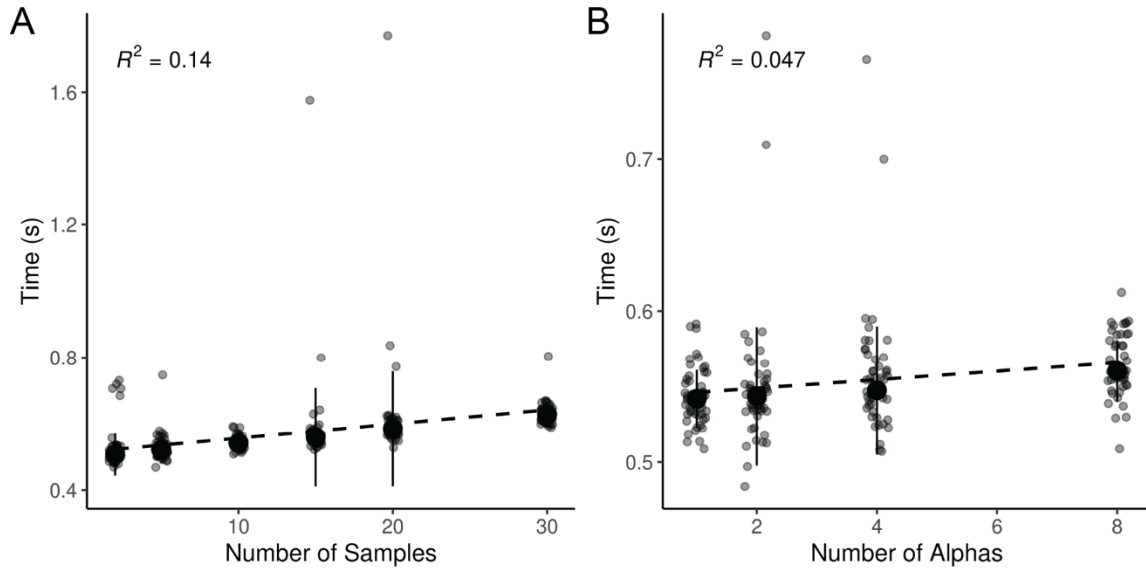
75 *Figure S2. Additional PERMANOVA results when using  $GU^A$  across a range of  $\alpha$  values.*  
76 PERMANOVAs were run testing the significance of two-three category groups from each  
77 dataset (provided in italics beneath data names). Results indicate *pseudo-F* statistics and *p*-values  
78 after 1,000 iterations. In the cooling reactor, only samples from Reactor cycle 1 were used; in the  
79 mouse gut, only stool samples were used, and in the soil, only mature samples were used. Note  
80 the y-axes for *pseudo-F* plots are variable between datasets, and y-axes for the *p*-value plots are  
81 log-scaled.

82

83



84 *Figure S3. Principal Coordinate Analysis ordinations of each dataset using  $U^R$  and  $U^A$ .* Points  
 85 are colored using the same categorical variable tested in the PERMANOVAs of Fig. 2 and Fig.  
 86 S2 (for additional details on experimental design, see [1, 3, 4, 15]). Both  $U^R$  and  $U^A$  were  
 87 calculated at an  $\alpha = 1$ .



89

90 *Figure S4. Additional parameters which weakly influence computation time for  $GU^4$ .* A)  $GU^4$   
91 was calculated 50 times across six sample sizes (2, 5, 15, 20, 30) with a constant of 2,000 ASVs  
92 and one calculated  $\alpha$  (though unweighted Unifrac is also calculated by default). B)  $GU^4$  was  
93 calculated 50 times across four alpha parameter sizes (1, 2, 4, 8; note unweighted Unifrac is also  
94 calculated by default) with a constant of 2,000 ASVs and 10 samples. In both panels,  $R^2$  is  
95 derived from a linear model between the x and y axes.

96

Package/Software	Version	Citation
R	4.5.0	[16]
RStudio	2024.12.1+563	[17]
tidyverse	2.0.0	[18]
phyloseq	1.52.0	[10]
vegan	2.7-1	[12]
GUniFrac*	1.8.1	[13]
ggtree	3.16.0	[19]
patchwork	1.3.1	[20]
NatParksPalettes	0.2.0	[21]
ape	5.8-1	[9]
broom	1.0.8	[22]
corrr	0.4.4	[23]
renv	1.0.5	[24]
microbenchmark	1.5.0	[14]
ggpubr	0.6.1	[25]
dada2	1.36.0	[5]
MAFFT	7.520	[7]
FastTree	2.1.11	[8]
cutadapt	5.1	[26]
extraDistr	1.10.0	[11]

97 *Table S1. Software and packages used in analysis.* Note that GUniFrac was modified slightly to  
 98 make incorporating absolute abundances more apparent; this version can be installed via Github  
 99 at <https://github.com/MarschmiLab/GUniFrac>.

100

101 **Supporting References**

- 102 1. Zhang K et al. Absolute microbiome profiling highlights the links among microbial  
103 stability, soil health, and crop productivity under long-term sod-based rotation. *Biol Fertil  
104 Soils* 2022;58:883–901. <https://doi.org/10.1007/s00374-022-01675-4>
- 105 2. Props R et al. Measuring the biodiversity of microbial communities by flow cytometry.  
106 *Methods in Ecology and Evolution* 2016;7:1376–1385. [https://doi.org/10.1111/2041-210X.12607](https://doi.org/10.1111/2041-<br/>107 210X.12607)
- 108 3. Pendleton A, Wells M, Schmidt ML. Upwelling periodically disturbs the ecological  
109 assembly of microbial communities in the Laurentian Great Lakes. 2025. *bioRxiv*, 2025. ,  
110 2025.01.17.633667
- 111 4. Barlow JT, Bogatyrev SR, Ismagilov RF. A quantitative sequencing framework for absolute  
112 abundance measurements of mucosal and luminal microbial communities. *Nat Commun*  
113 2020;11:2590. <https://doi.org/10.1038/s41467-020-16224-6>
- 114 5. Callahan BJ et al. DADA2: High-resolution sample inference from Illumina amplicon data.  
115 *Nat Methods* 2016;13:581–583. <https://doi.org/10.1038/nmeth.3869>
- 116 6. Quast C et al. The SILVA ribosomal RNA gene database project: improved data processing  
117 and web-based tools. *Nucleic Acids Research* 2013;41:D590–D596.  
118 <https://doi.org/10.1093/nar/gks1219>
- 119 7. Katoh K, Standley DM. MAFFT Multiple Sequence Alignment Software Version 7:  
120 Improvements in Performance and Usability. *Molecular Biology and Evolution*  
121 2013;30:772–780. <https://doi.org/10.1093/molbev/mst010>
- 122 8. Price MN, Dehal PS, Arkin AP. FastTree 2 – Approximately Maximum-Likelihood Trees  
123 for Large Alignments. *PLOS ONE* 2010;5:e9490.  
124 <https://doi.org/10.1371/journal.pone.0009490>

- 125 9. Paradis E et al. *ape*: Analyses of phylogenetics and evolution. 2023.
- 126 10. McMurdie PJ, Holmes S. *phyloseq*: An R package for reproducible interactive analysis and  
127 graphics of microbiome census data. *PLoS ONE* 2013;8:e61217.
- 128 11. Wolodzko T. *extraDistr*: Additional univariate and multivariate distributions. 2023.
- 129 12. Oksanen J et al. *vegan*: Community ecology package. 2022.
- 130 13. Chen J et al. Associating microbiome composition with environmental covariates using  
131 generalized UniFrac distances. *Bioinformatics* 2012;28:2106–2113.  
132 <https://doi.org/10.1093/bioinformatics/bts342>
- 133 14. Mersmann O. *microbenchmark*: Accurate timing functions. 2024.
- 134 15. Props R et al. Absolute quantification of microbial taxon abundances. *ISME J* 2017;11:584–  
135 587. <https://doi.org/10.1038/ismej.2016.117>
- 136 16. R Core Team. R: A language and environment for statistical computing. Vienna, Austria: R  
137 Foundation for Statistical Computing, 2022.
- 138 17. RStudio Team. RStudio: Integrated Development Environment for R. Boston, MA:  
139 RStudio, PBC., 2020.
- 140 18. Wickham H. *tidyverse*: Easily install and load the tidyverse. 2023.
- 141 19. Xu S et al. *Ggtree*: A serialized data object for visualization of a phylogenetic tree and  
142 annotation data. *iMeta* 2022;1:e56. <https://doi.org/10.1002/imt2.56>
- 143 20. Pedersen TL. *patchwork*: The composer of plots. 2024.
- 144 21. Blake K. *NatParksPalettes*: Color palettes inspired by national parks. 2022.
- 145 22. Robinson D, Hayes A, Couch S. *broom*: Convert statistical objects into tidy tibbles. 2023.
- 146 23. Kuhn M, Jackson S, Cimentada J. *corrr*: Correlations in R. 2022.
- 147 24. Ushey K, Wickham H. *renv*: Project environments. 2024.

- 148 25. Kassambara A. *ggpubr: ggplot2 based publication ready plots*. 2023.
- 149 26. Martin M. *Cutadapt removes adapter sequences from high-throughput sequencing reads*.
- 150 *EMBnet.journal* 2011;17:10–12. <https://doi.org/10.14806/ej.17.1.200>
- 151